Laser optogalvanic study of HCO $\tilde{A}$ state predissociation

R. Vasudev and R. N. Zare

Department of Chemistry, Stanford University, Stanford, California 94305
(Received 12 February 1982; accepted 15 February 1982)

Widths of lines in the (0, 9^0, 0)–(0, 0^1, 0) band of the HCO $\tilde{A}\,^2A''$–$\tilde{X}\,^2A'$ transition are recorded using a single-mode dye laser, revealing a strong dependence on the rotational quantum number N. The HCO radical is produced in a radio frequency discharge in acetaldehyde (CH_3CHO) vapor and the $\tilde{A}$–$\tilde{X}$ transition in the 570–630 nm region is detected by laser-induced changes in the discharge impedance. The variation of widths with N is interpreted in terms of Coriolis interaction and K-type resonance of the (0, 9^0, 0)$\Sigma(K'=0)$ level with nearby strongly predissociated $\Pi(K'=1)$ and $\Delta(K'=2)$ levels, respectively, of the upper state.

INTRODUCTION

Although the formyl radical HCO had been postulated for a long time as an important reaction intermediate, direct spectroscopic study of HCO was impeded by the difficulty of obtaining a sufficiently high concentration of this reactive species. The first high-resolution studies of HCO were carried out by Ramsay,[1] Herzberg and Ramsay,[2] and Johns, Priddle, and Ramsay,[3] who photographed the absorption spectrum of the HCO red bands extending from 460 to 860 nm, following the flash photolysis of acetaldehyde. The HCO red bands were identified as transitions between the $\tilde{A}\,^2A''$ and $\tilde{X}\,^2A'$ states, which are split by strong Renner–Teller interaction.[4] This Renner–Teller pair correlates with a $^2\Pi$ state in the limit of linear geometry. The equilibrium geometry of the lower state ($\tilde{X}\,^2A'$) is definitely bent, while that of the upper state ($\tilde{A}\,^2A''$) is linear (or nearly linear).

For HCO as well as DCO, most of the levels of the excited state are diffuse. The absorption spectrum consists mainly of a long progression of bands (0, v_2', 0)–(0, 0, 0) involving the bending vibration v_2' of the excited state. Alternate bands in the progression appear sharp. The sharp bands involve the $K''=1$ rotational levels of the ground state and the $K'=0$ levels of the excited state. Hence, the vibronic symmetry of the excited state is either $^2\Sigma^+$ or $^2\Sigma^-$. The latter assignment is preferred because a $^2\Sigma^-$ excited state cannot correlate with $H(^2S)+CO(^1\Sigma^+)$. This assignment establishes $^2A'$ as the ground state of the formyl radical.

By trapping HCO in matrices of CO, the rare gases, or in single cyrstals of formic acid, both the infrared[5–7] and electron spin resonance[8–10] (ESR) spectra of the ground state of the formyl radical have been recorded. This has permitted the determination of the frequencies of the vibrational fundamentals and the elements of the g tensor and the hyperfine tensors for the proton, the deuteron, and ^{13}C. In addition, it has also proved possible to obtain the microwave spectrum of free HCO radicals by pumping a reaction mixture of fluorine atoms and formaldehyde (CH_2O) through the cavity of a microwave spectrometer.[11–17] This had led to a determination of the elements of the spin-rotation tensor, as well as very accurate values for two of the three moments of inertia of the ground state. Brown and Ramsay[18] reinvestigated the HCO visible spectrum and found some very weak $\Delta K=2$ lines from which a direct measurement of the remaining ground state moment of inertia could be made. From these measurements the equilibrium geometry for the HCO $\tilde{X}$ state is deduced to be $r_{CH}=1.125(5)$ Å, $r_{CO}=1.175(1)$ Å, and $\theta_{HCO}=124.95(25)^\circ$.

The HCO radical has also been spectroscopically studied using laser magnetic resonance[18–22] and laser electric resonance.[23] These investigations have determined the major molecular parameters for HCO in the (0, 1, 0) level of the $\tilde{X}$ state, as well as the value of the electric dipole moments in the (0, 0, 0) and (0, 1, 0) levels. Although the HCO $\tilde{A}$–$\tilde{X}$ system has only been observed in absorption, HCO shows a complex series of emission bands between 250 and 410 nm, which are characteristic of hydrocarbon–oxygen flames.[24,25] A partial rotational analysis of these so-called hydrocarbon flame bands has been completed,[26–28] but does not add substantially to our knowledge of the HCO $\tilde{X}$ or $\tilde{A}$ states. The HCO radical can also be observed by intracavity gain spoiling of a broadband dye laser,[29–31] but so far, this technique has been applied primarily to understand HCO appearance rates, vibrational relaxation, and reaction kinetics following pulsed photolysis of formaldehyde or acetaldehyde.

Many of the well established laser detection techniques cannot be used to study the $\tilde{A}$–$\tilde{X}$ system of HCO. Laser-induced fluorescence, for example, is normally a powerful tool but is inapplicable here due to the very low fluorescence quantum yield of the $\tilde{A}$ state. In this paper, we report the detection and spectroscopy of the HCO $\tilde{A}$–$\tilde{X}$ transition by exploiting the optogalvanic effect.[32] The laser optogalvanic (LOG) technique relies on impedance changes accompanying laser excitation of species in discharges and flames. Although almost all studies to date have been made on atoms, molecular systems are beginning to receive attention.[33–37] Recent experiments suggest that the optogalvanic effect is especially large when the pumped transition involves excitation of Rydberg states or, in the case of molecules, predissociated states. Compared to the conventional flash-photolysis absorption technique, LOG detection of HCO, as described in this paper, requires about 10^5 times smaller quantity of the parent acetaldehyde molecule.

Almost all laser optogalvanic studies to date have involved dc discharges.[32] However, our attempt to apply this method failed because of carbonization of electrodes, resulting in arcing. We overcame this problem by using

 0021-9606/82/115267-04$02.10

an electrodeless rf discharge.[37,38] The HCO LOG spectrum has been recorded by using a rhodamine 6G dye laser to cover the 580–620 nm region. Scans with a single-mode dye laser over the $(0, 9°, 0)$–$(0, 0^1, 0)$ band show an N-dependent linewidth which is much broader than the Doppler width. Various predissociation mechanisms are discussed. It is proposed that interaction of the upper state $\Sigma(K'=0)$ level with neighboring, strongly predissociated $\Pi(K'=1)$ and $\Delta(K'=2)$ levels can explain the heterogeneous part of the predissociation widths (rates).

EXPERIMENTAL

The present experimental setup is essentially the same as that very recently used by Lyons *et al.* for the LOG detection of the $2p_2$–$1s_5$ transition of neon.[38] Briefly, the HCO radical is produced in an rf discharge through acetaldehyde, mixed with argon/helium for sustaining the discharge (total pressure ~1.5 Torr). The rf discharge is driven by an RCA 6AF4A triode. Impedance changes accompanying laser excitation of HCO are detected by the reaction of the oscillator. The 12-turn rf coil is 2 cm in length. The rf generated (~30 MHz and 1–10 W) sustains a ~1 cm long discharge, initiated by a tesla coil.

For detection of low resolution HCO spectra, an Ar^+ laser-pumped dye laser (Coherent Raidation CR 599-21) is used multimode (bandwidth ~30 GHz). High-resolution spectra are measured using a single-mode dye laser (bandwidth ~1 MHz). The dye laser beam in both cases is mechanically chopped and the ac signal across an 8 $k\Omega$ resistor is separated from dc background by an 0.02 μF capacitor, processed by a lock-in amplifier and displayed on a stripchart recorder. The low-resolution spectra are calibrated by simultaneously recording a dc optogalvanic spectrum of neon. For the high-resolution scans, fluorescence excitation spectra of I_2 and fringes from a calibrated etalon are used.[39]

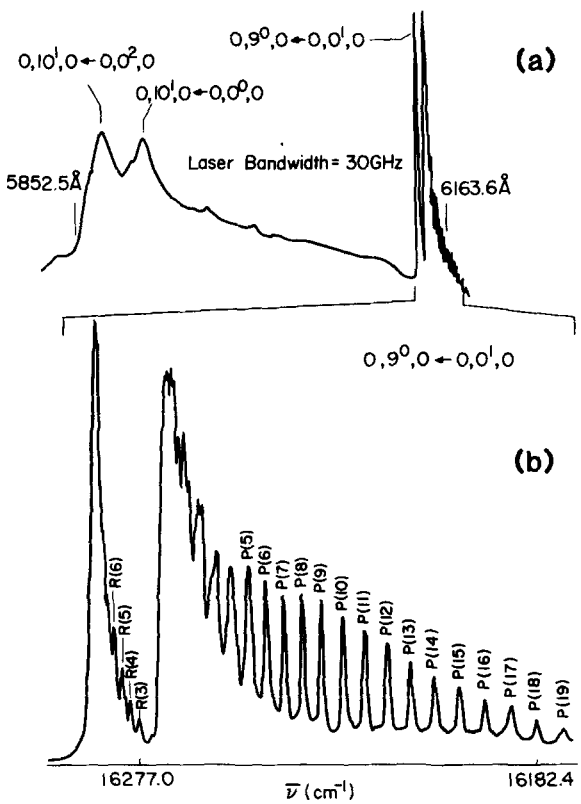

FIG. 1. Low-resolution laser optogalvanic spectra of the HCO $\tilde{A}$–$\tilde{X}$ system recorded (a) over the 580–620 nm region at a scan speed of 1.8 nm/min; and (b) over the $(0, 9^0, 0)$–$(0, 0, 0)$ band at a scan speed of 0.14 nm/min.

FIG. 2. High-resolution laser optogalvanic trace of the $Q(5)$ line of the HCO $\tilde{A}(0, 9^0, 0)$–$\tilde{X}(0, 0^1, 0)$ band. The lower trace shows the simultaneous recording of the fluorescence excitation of I_2, as well as fringes from a 1.97 GHz etalon used for calibrating the wavelength. The wave numbers 16 267.801 3 and 16 268.022 1 cm^{-1} attached to the I_2 calibration lines on the left side of Fig. 2 should be interchanged.

RESULTS AND DISCUSSION

Figure 1 shows the low-resolution $\tilde{A}$–$\tilde{X}$ LOG spectrum of HCO, taken in the rhodamine 6G region. Near 613.8 nm, the signal-to-noise ratio is in excess of 10^3, which is limited by fluctuations in the laboratory surroundings rather than by the instruments used. Here LOG detection requires only 2×10^{-5} m atm of the parent acetaldehyde molecules, whereas flash photolysis/absorption techniques need up to 4 m atm of the parent. In Fig. 1(a), the broad features to the blue correspond to transitions terminating on the strongly predissociated $(0, 10^1, 0)$ Π level from $K''=0$ and 2 levels of the $(0, 0, 0)$ ground state. The estimated rotational linewidths[3] are 20 cm^{-1}, corresponding to a predissociation lifetime of about 0.3 ps. To the red in Fig. 1(a) is a much sharper feature at 613.8 nm. This is identified as the $(0, 9^0, 0)$–$(0, 0^1, 0)$ transition, which is shown at a slower scan rate in Fig. 1(b). Even in this low-resolution spectrum, an N-dependent line broadening is discernible, although it is convoluted with the ~30 GHz laser bandwidth.

The linewidths of individual rotational lines are measured with a single-mode dye laser (bandwidth ~1 MHz). A typical trace is shown in Fig. 2. The variation of the

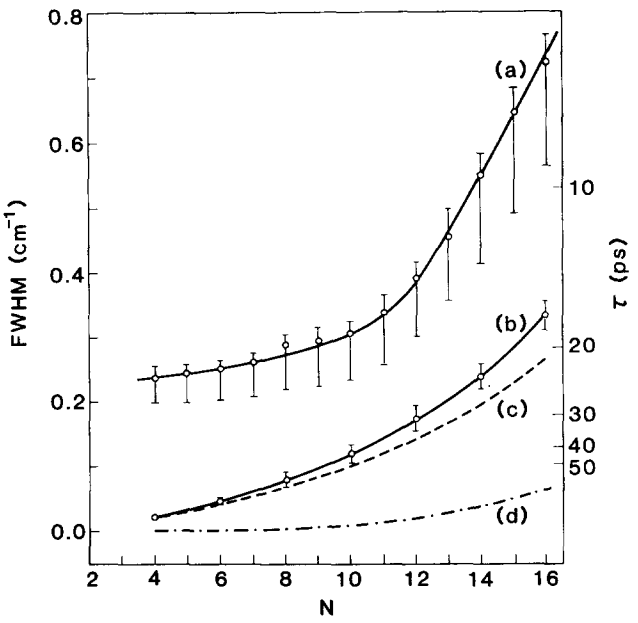

FIG. 3. Variation of excited state linewidth with rotational quantum number N' showing (a) the observed measurements, and (b) the sum of Coriolis interaction given in (c) and K-type resonance given in (d). Comparison of (a) to (b) shows that the heterogeneous (N'-dependent) part of the predissociation mechanism is well described by combined action of the above two perturbations but there is a homogeneous (N'-independent) part that is unaccounted for.

linewidth with the rotational quantum number N' is plotted in Fig. 3. Here, each width represents the average of measurements from all three branches. The larger uncertainty in the upper confidence limit at high N' mainly reflects the difficulty in estimating the baseline, since the line profile extends somewhat beyond the scan range (30 GHz) of the laser. The entire profile is thus obtained by piecing together two or more scans.

It is known from the work of Brown and Ramsay[18] that the spin splitting is seen only in the $R(1)$ line, originating predominantly from the splitting in the ground state. Moreover, the low frequency component of this doublet is slightly stronger. Examination of the single-mode scan of the $Q(5)$ line, for example, shows a slight asymmetry which is consistent with the low frequency component being more intense, with a doublet separation of ~ 0.06 cm^{-1} and a linewidth of ~ 0.19 cm^{-1}. The point we wish to emphasize here is that the actual widths of individual transitions are somewhat less than the observed widths because of spin doubling. Rough calculations show that for two lines to be superimposed in such a way that there is a dip in between the maxima, the widths of individual components must be $\geq 75\%$ of the width of the blended line. The slight asymmetry, shown in Fig. 2, is not seen at higher N' values, due to more rapid predissociation rates. However, since the variation of the excited state spin splitting with N' is not known, we use the absence of a dip in the line profile to estimate the lower confidence limit for high N' widths, as explained above. For low N' lines, a slight complication is the convolution of the natural (Lorentzian) with Doppler (Gaussian) profiles to yield a Voigt profile.[40] Thus one needs, in principle, to extract the natural width from the observed profile. Deconvolution from a Voigt profile with FWHM $= 0.22$ cm^{-1}, e.g., gives a natural linewidth of ~ 0.20 cm^{-1} (assuming a Doppler width [(FWHM) of 0.05 cm^{-1}]. However, in view of other uncertainties we ignore this effect. In any case, for high N', such a correction is insignificant.

We now consider the mechanisms responsible for the observed predissociation. The width Γ_Σ of a $\Sigma(K'=0)$ level due to interaction with a strongly predissociated level p is

$$\Gamma_\Sigma = \frac{\langle \Sigma | H_{\rm int} | p \rangle^2}{(E_\Sigma - E_p)^2} \Gamma_p \,, \tag{1}$$

where $H_{\rm int}$ is a term in the Hamiltonian that couples $|\Sigma\rangle$ to $|p\rangle$, Γ_p is the width of the perturbing level, and $(E_\Sigma - E_p)$ is the energy separation between the two. The following heterogeneous interactions may play a role: (i) Perturbation with Δ levels, through K-type resonance; (ii) Perturbation with Π levels, through Coriolis interaction.

Interaction (i) has been invoked by Brown and Ramsay[18] to explain (1) the trend towards negative centrifugal distortion coupling constants D' with increasing v_2' of Σ levels, and (2) the widths of the $(0, 13^0, 0)$ levels of the $\tilde{A}$ state. The apparent D' due to such an effect is given by

$$D'_{\rm app} = D'_{000} - \frac{4B^4}{\omega_2^2}\left(1 + \frac{\zeta_{23}^2\omega_2^2}{\omega_3^2 - \omega_2^2}\right)^2 \times \left\{\frac{(v_2+1) + [(v_2-1)(v_2+3)]^{1/2}}{32(E_\Sigma - E_\Delta)}\right\}^2 , \tag{2}$$

where ζ_{23} is a Coriolis coupling constant. Hence, the linewidth due to this interaction has the form

$$\Gamma_\Sigma = |\Delta D'| \frac{[N'(N'+1)]^2}{(E_\Sigma - E_\Delta)} \Gamma_\Delta \,, \tag{3}$$

where $\Delta D' = D'_{\rm app} - D'_{000}$. The calculated values of Γ_Σ for the $(0, 9^0, 0)$ level due to this interaction with $(0, 9^2, 0)$ are shown in Fig. 3 as curve (d).

Interaction (ii) connects Σ and Π levels by x, y Coriolis interaction.[41] The wave functions[42,43] for Σ and Π vibronic levels in a Π electronic state, in the presence of Renner–Teller coupling, are

$$\psi(\Sigma^\pm) = (1/\sqrt{2})(|v_2, v_n, -1, 0, J\rangle \pm |v_2, v_n, +1, 0, J\rangle) \tag{4}$$

and

$$\psi(\Pi) = \tfrac{1}{2}[(|v_2, v_n, 0, 1, J\rangle + |v_2, v_n, +2, 1, J\rangle) \pm (|v_2, v_n, 0, -1, J\rangle + |v_2, v_n, -2, -1, J\rangle)] \,, \tag{5}$$

where the basis functions are labeled by $|v_2, v_n, l, K, J\rangle$, v_n being the quantum number associated with a stretching mode. Here, l and K are signed quantum numbers. The Coriolis operator[41] which couples $\Sigma(|K| = 0)$ and $\Pi(|K| = 1)$ levels is given by

$$H^{\rm Cor} = 2B(-p_x N_x - p_y N_y) = -B(p_- N_+ - p_+ N_-) \,, \tag{6}$$

where p_x, p_y and N_x, N_y are the projections of vibration-

al and rotational angular momenta, respectively, on the x, y axes of the molecule. The vibrational selection rules for x, y Coriolis interaction are $\Delta v_2 = \pm 1$ and $\Delta v_n = \pm 1$. For the case at hand, i.e., $(0, 9^0, 0)$ interacting with Π levels, only the $(0, 8^1, 1)$ level contributes to a significant extent because of its proximity. The relevant matrix elements for $p_\pm$ are tabulated by Johns.[43]

The contribution of such an interaction with $(0, v_2^1, 1)$ to the $(0, v_2 + 1^0, 0)$ widths is given by

$$\Gamma_\Sigma = \tfrac{1}{2}(v_2+1)\,\frac{(\omega_3+\omega_2)^2}{\omega_2\omega_3}\,\zeta_{23}^2 B^2[N'(N'+1)]\,\frac{\Gamma_\Pi}{(E_\Sigma - E_\Pi)^2}\,, \quad (7)$$

where ζ_{23} is a Coriolis coupling constant, $(E_\Sigma - E_\Pi)$ is the $(0, 8^1, 1)$–$(0, 9^0, 0)$ separation, and Γ_Π is the width of the Π levels.

The widths calculated from this expression are shown in curve (c) of Fig. 3. Also shown, as curve (b), is the width resulting from the sum of mechanisms (i) and (ii). The error bars in curve (b) originate from the estimated uncertainty of ± 3 cm^{-1} in Γ_Π. The variation of curve (b) with N' appears to reproduce the observed trend in the measured widths. Granted this, the approximately constant difference between curves (c) and (d) must then be ascribed to homogeneous (e.g., spin-orbit) interactions with other short-lived levels (e.g., the high-lying levels of the ground state). To explore this matter further, it is suggested that the widths of the $(0, 1^0, 0)$ level of the $\tilde{A}$ state be measured, since the heterogeneous perturbation for this level are expected to be rather small. However, a transition to this level from the vibrationless ground state is expected to have an extremely small Franck–Condon factor and, in addition, would require laser excitation near 990 nm, which unfortunately is not a convenient laser wavelength.

In summary, the present study concerns the laser optogalvanic measurement of predissociation rates of the $\tilde{A}$ state of HCO produced in an rf discharge. The ease with which these measurements can be carried out suggests that this technique may be used to advantage in studying nonradiative processes in other species that can be produced only in low concentrations.

ACKNOWLEDGMENTS

We thank G. -Y. Yan for making available to us a preprint of Ref. 38. This work is supported by the National Science Foundation under NSF CHE-80-06524.

[1] D. A. Ramsay, J. Chem. Phys. **21**, 960 (1953).
[2] G. Herzberg and D. A. Ramsay, Proc. R. Soc. London Ser. A **233**, 34 (1956).
[3] J. W. C. Johns, S. H. Priddle, and D. A. Ramsay, Discuss. Faraday Soc. **35**, 90 (1963).
[4] D. A. Ramsay, *Advances in Spectroscopy*, edited by H. W. Thompson (Interscience, New York, 1959), Vol. 1, p. 1.
[5] G. E. Ewing, W. E. Thompson, and G. C. Pimentel, J. Chem. Phys. **32**, 927 (1960).
[6] D. E. Milligan and M. E. Jacox, J. Chem. Phys. **41**, 3032 (1964).
[7] J. F. Ogilvie, Spectrochim. Acta Part A **23**, 737 (1967).
[8] F. J. Adrian, E. L. Cochran, and V. A. Bowers, J. Chem. Phys. **36**, 1661 (1962).
[9] E. L. Cochran, F. J. Adrian, and V. A. Bowers, J. Chem. Phys. **44**, 4626 (1966).
[10] R. W. Holmberg, J. Chem. Phys. **51**, 3255 (1969).
[11] I. C. Bowater, J. M. Brown, and A. Carrington, J. Chem. Phys. **54**, 4957 (1971).
[12] I. C. Bowater, J. M. Brown, and A. Carrington, Proc. R. Soc. London Ser. A **333**, 265 (1973).
[13] P. S. H. Bolman, J. M. Brown, A. Carrington, and G. J. Lycett, Proc. R. Soc. London Ser. A **335**, 113 (1973).
[14] S. Saito, Astrophys. J. **178**, L95 (1972).
[15] J. A. Austin, D. H. Levy, C. A. Gottlieb, and H. E. Radford, J. Chem. Phys. **60**, 207 (1974).
[16] B. J. Boland, J. M. Brown, and A. Carrington, Mol. Phys. **34**, 453 (1977).
[17] B. J. Boland, J. M. Brown, A. Carrington, and A. C. Nelson, Proc. R. Soc. London Ser. A **360**, 507 (1978).
[18] J. M. Brown and D. A. Ramsay, Can. J. Phys. **53**, 2232 (1975).
[19] J. M. Cook, K. M. Evenson, C. J. Howard, and R. F. Curl, Jr., J. Chem. Phys. **64**, 1381 (1976).
[20] J. M. Brown, J. Buttenshaw, A. Carrington, and C. R. Parent, Mol. Phys. **33**, 589 (1977).
[21] J. W. C. Johns, A. R. W. McKellar, and M. Riggin, J. Chem. Phys. **67**, 2427 (1977); Faraday Discuss. Chem. Soc. **71**, 63 (1981).
[22] J. M. Brown, J. Buttenshaw, A. Carrington, K. Dumper, and C. R. Parent, J. Mol. Spectrosc. **79**, 47 (1980).
[23] B. M. Landsberg, A. J. Merer, and T. Oka, J. Mol. Spectrosc. **67**, 459 (1977).
[24] W. M. Vaidya, Proc. R. Soc. London Ser. A **147**, 513 (1934); Proc. Phys. Soc. London Sect. A **64**, 428 (1951); Proc. R. Soc. London Ser. A **279**, 572 (1964).
[25] P. J. Dyne and D. W. G. Style, Discuss. Faraday Soc. **2**, 159 (1947).
[26] D. E. Milligan and M. E. Jacox, J. Chem. Phys. **51**, 277 (1969).
[27] R. N. Dixon, Trans. Faraday Soc. **65**, 3141 (1969).
[28] M. E. Jacox, Chem. Phys. Lett. **56**, 43 (1978).
[29] J. H. Clark, C. B. Moore, ane J. P. Reilly, Int. J. Chem. Kinet. **10**, 427 (1978).
[30] J. P. Reilly, J. H. Clark, C. B. Moore, and G. C. Pimentel, J. Chem. Phys. **69**, 4381 (1978).
[31] R. J. Gill and G. H. Atkinson, Chem. Phys. Lett. **64**, 426 (1979).
[32] J. E. M. Goldsmith and J. E. Lawler, Contemp. Phys. **22**, 235 (1981).
[33] P. K. Schenk, W. G. Mallard, J. C. Travis, and K. C. Smyth, J. Chem. Phys. **69**, 5147 (1978).
[34] D. Feldmann, Opt. Commun. **29**, 67 (1979).
[35] C. T. Rettner, C. R. Webster, and R. N. Zare, J. Phys. Chem. **85**, 1105 (1981).
[36] C. Demuynck and L. L. Destombes, IEEE J. Quantum Electron. **17**, 575 (1981).
[37] T. Suzuki, Opt. Commun. **38**, 364 (1981).
[38] D. R. Lyons, A. L. Schawlow, and G.-Y. Yan, Opt. Commun. **38**, 35 (1981).
[39] S. Gerstenkorn and P. Luc, *Atlas du Spectre d'Absorption de la Molécule d'Iode* (C.N.R.S., Paris, 1978).
[40] B. R. Armstrong, J. Quant. Spectrosc. Radiat. Transfer **7**, 61 (1967).
[41] I. M. Mills, Pure Appl. Chem. **11**, 325 (1965).
[42] J. A. Pople and H. C. Longuet-Higgins, Mol. Phys. **1**, 372 (1958).
[43] J. W. C. Johns, J. Mol. Spectrosc. **15**, 473 (1965).